International Journal of Science and Research (IJSR)
ISSN (Online): 2319-7064
Impact Factor (2012): 3.358

Thermodynamic and Adsorption Behavior of eco-Friendly Purine Derivatives on the Corrosion of Carbon Steel in 1 M HCl

Ahmed A. Farag[1], Khalid Zakaria[2]

[1]Petroleum Applications Department, Egyptian Petroleum Research Institute (EPRI)
1 Ahmed El-Zomor St., Nasr City, 11727, Cairo, Egypt

[2]Analysis and Evaluation Department, Egyptian Petroleum Research Institute (EPRI)
1 Ahmed El-Zomor St., Nasr City, 11727, Cairo, Egypt

Abstract: ***The behavior of carbon steel in 1.0 mol dm^{-3} HCl in the presence of novel purine inhibitors namely 1H-pyrazolo[3,4-d]pyrimidin-4(2H)-one (PPO) and 6-[(1-methyl-4-nitro-5-imidazolyl)sulfanyl]purine (ISP) in the concentration range ($1\times10^{-4} - 5\times10^{-3}$ mol dm^{-3}) was studied using weight loss, open circuit potential, potentiodynamic polarization electrochemical impedance spectroscopy (EIS) and scanning electron microscopy (SEM) techniques. Potentiodynamic polarization shows that PPO and ISP act as mixed-type inhibitors. The values of the activation energy, equilibrium constant, free energy of adsorption, activation enthalpy and activation entropy were discussed. The adsorption of inhibitors on metal followed Langmuir's adsorption isotherm. The values of suggest the chemical adsorption of PPO and ISP on carbon steel surface.***

Keywords: Carbon steel, Acid corrosion, EIS, Polarization, SEM

1. Introduction

Hydrochloric acid (HCl) solutions are widely used in the industry, some of the important fields of application being acid pickling of iron and steel, chemical cleaning and processing, ore production and oil well acidification [1]. Because of the general aggression of acid solutions, inhibitors are commonly used to reduce the corrosive attack on metallic materials. Most well-known acid inhibitors are organic compounds containing nitrogen, sulfur, and oxygen atoms. Among them, nitrogen containing heterocyclic compounds is considered to be effective corrosion inhibitors for steel in acid media [2]. N-heterocyclic compound inhibitors act by adsorption on the metal surface, and the adsorption of N-heterocyclic inhibitor takes place through nitrogen heteroatom, as well as those with triple or conjugated double bonds or aromatic rings in their molecular structures. Although N-heterocyclic organic compounds have good anti-corrosive activity; they are highly toxic to both human beings and environment [3].

The safety and environmental issues of corrosion inhibitors arisen in industries has always been a global concern. These toxic effects have led to the use of eco-friendly and harmless N-heterocyclic compounds as inhibitors. As an important N-heterocyclic compound, purine and purine derivatives are non-toxic and biodegradable; this makes the investigation of their inhibiting properties significant within the context of the current priority to produce eco-friendly inhibitors.

However, data on the use of purine and purine derivatives as corrosion inhibitors are not so plentiful. The aim of this work is to investigate a novel purine inhibitors namely, 1H-pyrazolo[3,4-d]pyrimidin-4(2H)-one (PPO) and 6-[(1-methyl-4-nitro-5-imidazolyl)sulfanyl]purine (ISP) (Figure 1) as the corrosion inhibitor for carbon steel in 1 M HCl using different techniques.

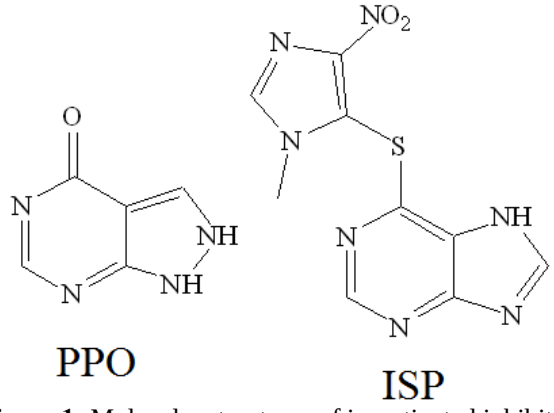

Figure 1: Molecular structures of investigated inhibitors

2. Experimental

2.1. Material

Tests were performed on carbon steel of the following composition (wt.%): 0.07% C, 0.24% Si, 1.35% Mn, 0.017% P, 0.005% S, 0.16% Cr, 0.18% Ni, 0.12% Mo, 0.01% Cu and the remainder Fe.

2.2. Solutions

The inhibitors solutions with different concentrations were prepared in 1.0 mol dm^{-3} HCl. The corrosion tests were performed in HCl solution in the absence and presence of various concentrations of inhibitors. The aggressive solution of 1.0 mol dm^{-3} HCl was prepared by dilution of analytical grade 37% HCl with distilled water. For each experiment, a freshly prepared solution was used under air atmosphere without stirring at 298 K.

2.3. Gravimetric measurements

The carbon steel coupons of 7.0 cm × 2.0 cm × 0.03 cm were abraded with a series of emery paper beginning from 400 to 1200, degreased with acetone, rinsed with distilled water and dried in hot air. After weighing accuracy, the specimens were immersed in 150 ml beaker, which contained 150 ml hydrochloric acid with and without the addition of various concentrations of inhibitors. All the aggressive acid solutions were open to air. After 24 h, the specimens were taken out, washed, dried, and weighed accurately. In order to get good reproducibility, the experiments were carried out in triplicate, and the average weight loss of three parallel carbon steel coupons was reported. Then the tests were repeated at different temperatures. The corrosion rate (ν) was calculated from the following equation:

$$\nu = \frac{W}{St} \quad (1)$$

where W is the average weight loss of three parallel carbon steel coupons, S the total area of one steel coupon, and t is immersion time (24 h). With the calculated corrosion rate, the inhibition efficiency (η_g) of inhibitors on the corrosion of carbon steel was calculated as follows [4]:

$$\eta_g = \frac{\nu_0 - \nu}{\nu_0} \times 100 \quad (2)$$

where ν_0 and ν are the values of the corrosion rate without and with the addition of the inhibitor, respectively.

2.4. Electrochemical measurements

The electrochemical measurements were carried out using Volta lab 40 (Tacussel-Radiometer PGZ301) potentiostate and controlled by Tacussel corrosion analysis software model (Voltamaster 4) at under static condition. The corrosion cell used had three electrodes. The reference electrode was a saturated calomel electrode (SCE). A platinum electrode was used as auxiliary electrode. Carbon steel coupons having the area of 1 cm^2 were used as a working electrode. The working electrode was immersed in test solutions for 30 minutes to a establish steady state open circuit potential (E_{ocp}). After measuring the E_{ocp}, the electrochemical measurements were performed. The EIS experiments were conducted in the frequency range with high limit of 10^5 Hz and different low limit 10^{-2} Hz at open circuit potential. The polarization curves were obtained in the potential range from −900 to −200 mV(SCE) with 0.5 mV s^{-1} scan rate.

3. Results and Discussion

3.1. Gravimetric measurements

3.1.1. Effect of inhibitor concentration

Table 1 showed the values of corrosion rates (mg cm^{-2} h^{-1}), surface coverage (θ) and inhibition efficiencies (η_g) obtained from gravimetric measurements in the absence and presence of various concentrations of inhibitors at 298 K for 24 h immersion in 1.0 mol dm^{-3} HCl. The variation of corrosion rates (ν) with inhibitor concentrations is shown in Figure 2.

Table 1: Gravimetric measurements parameters for carbon steel in 1.0 mol dm^{-3} HCl containing various concentrations of PPO and ISP at 298 K

Conc. (mol dm^{-3})	PPO			ISP		
	ν (mg cm^{-2} h^{-1})	θ	η_g (%)	ν (mg cm^{-2} h^{-1})	θ	η_g (%)
Blank	0.686	—	—	0.686	—	—
1×10^{-4}	0.482	0.297	29.7	0.321	0.532	53.2
5×10^{-4}	0.345	0.497	49.7	0.181	0.735	73.5
1×10^{-3}	0.220	0.679	67.9	0.084	0.878	87.8
5×10^{-3}	0.122	0.822	82.2	0.081	0.882	88.2

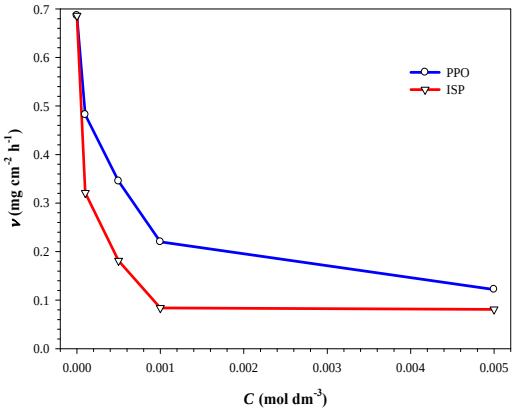

Figure 2: Relationship between the corrosion rate and inhibitor concentration for carbon steel at 298 K

It is clear that the weight loss decreased (i.e. ν is suppressed) and η_g increased with increasing concentration of inhibitors. The maximum η_g values of 5×10^{-3} mol dm^{-3} of PPO and ISP were found 82.2% and 88.2%, respectively. The inhibition of corrosion occurs due to the larger surface coverage (θ) of metal surface by inhibitor molecules [5].

3.1.2. Effect of temperature

Weight loss measurements were studied in the temperature range of 298–328 K in the absence and presence of 5×10^{-3} mol dm^{-3} of PPO and ISP during 24 h of immersion 5×10^{-3} mol dm^{-3}) of PPO and ISP. The results in Table 2 revealed that the corrosion rate (ν) increases with increase temperature in both uninhibited and inhibited solutions but the ν increases more rapidly with temperature in the absence of the inhibitor. It may be due to the fact that higher temperature accelerates the movement of the organic molecules and weakens the adsorption capacity of inhibitor on the metal surface. Dissolution of carbon steel is generally accompanied by evolution of hydrogen gas in acidic media and corrosion rate is accelerated by the increase in temperature, resulting in higher dissolution of the carbon steel. It is clear from the Table 2 that η_g decreases with increasing the solution temperature from 298 to 328 K. The decrease in η_g might be due desorption of the inhibitor molecules from the carbon steel surface.

Table 2: Gravimetric measurements parameters for carbon steel in 1.0 mol dm^{-3} HCl and containing optimum concentrations (5×10^{-3} mol dm^{-3}) of PPO and ISP at different temperatures

Temperature	Parameters	Blank	PPO	ISP
298 K	v (mg cm^{-2} h^{-1})	0.686	0.122	0.081
	θ	—	0.822	0.882
	η_g (%)	—	82.2	88.2
308 K	v (mg cm^{-2} h^{-1})	0.988	0.202	0.149
	θ	—	0.796	0.849
	η_g (%)	—	79.6	84.9
318 K	v (mg cm^{-2} h^{-1})	1.868	0.521	0.42
	θ	—	0.721	0.775
	η_g (%)	—	72.1	77.5
328 K	v (mg cm^{-2} h^{-1})	3.673	1.455	1.238
	θ	—	0.604	0.663
	η_g (%)	—	60.4	66.3

3.1.3. Adsorption isotherms

The values of surface coverage and inhibitor concentration were used to obtain the isotherms [6]. Various isotherms (Temkin, Frumkin and Langmuir isotherm) have been tested, but the best fit was obtained for Langmuir isotherm. The Langmuir isotherm is given by:

$$\frac{C}{\theta} = \frac{1}{K_{ads}} + C \qquad (3)$$

where C is the inhibitor concentration, θ is the surface coverage ($\theta = \eta_g / 100$), K_{ads} is the equilibrium constant of adsorption process. Plots of C/θ against C yield straight lines as shown in Figure 3, and the corresponding linear regression parameters are listed in Table 3.

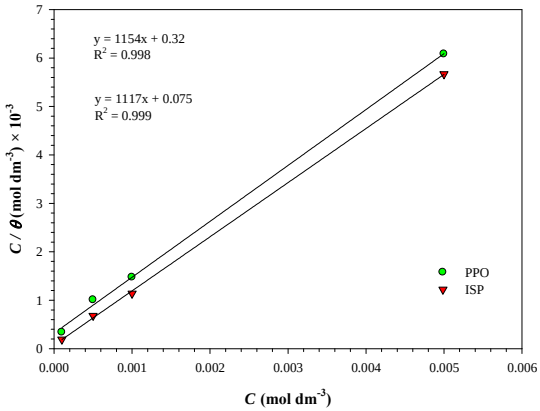

Figure 3: Langmuir adsorption plots of carbon steel in 1.0 mol dm^{-3} HCl containing the investigated inhibitors at 298 K

Both linear correlation coefficient (r) and slope are close to 1, indicating the adsorption of two inhibitors on the carbon steel surface obeys Langmuir adsorption isotherm. The adsorptive equilibrium constant (K_{ads}) can be calculated from the reciprocal of the intercept of C/θ–C curve. Generally, a large value of K_{ads} attribute to the stronger and more stable adsorbed layer formed on the metal surface. The standard free energy of adsorption (ΔG°_{ads}) can be given as the following equation:

$$\Delta G^{\circ}_{ads} = -RT\ln(55.5K_{ads}) \qquad (4)$$

where, R is the gas constant (8.314 J mol^{-1} K^{-1}), T the absolute temperature (K), and the value 55.5 is the concentration of water in solution expressed in molar.

Table 3: Adsorption equilibrium constant and standard free energy of adsorption of the investigated inhibitors for carbon steel in 1.0 mol dm^{-3} HCl solution at 298 K

Inhibitor	Slope	K_{ads} (M^{-1})	$-\Delta G^{\circ}_{ads}$ (kJ mol^{-1})
PPO	1.1	3.1 × 10^6	30.4
ISP	1.1	13.3 × 10^6	34.1

The high values of K_{ads} and negative values of ΔG°_{ads} suggested that, inhibitor molecules strongly adsorb on the carbon steel surface. Values of ΔG°_{ads} around −20 kJ mol^{-1} or lower are consistent with the electrostatic interaction between charged inhibitor molecules and the charged metal surface (physisorption); those around −40 kJ mol^{-1} or higher involve charge sharing or transfer from the inhibitor molecules to the metal surface to form a coordinate type of bond (chemisorption) [7]. The obtained ΔG°_{ads} values were −30.4 and −34.1 kJ mol^{-1} for PPO and ISP, respectively. This indicates that the adsorption takes place mainly through the electrostatic interaction between charged inhibitor molecules and the charged metal surface (physisorption).

3.1.4. Thermodynamic activation parameters

Arrhenius and transition state equations were used to know the dependence of corrosion rate on temperature:

$$v = A\exp\left(\frac{-E_a}{RT}\right) \qquad (5)$$

$$v = \frac{RT}{Nh}\exp\left(\frac{\Delta S^*}{R}\right)\exp\left(\frac{-\Delta H^*}{RT}\right) \qquad (6)$$

where A is the pre-exponential factor, E_a represents apparent activation energy, N is the Avogadro's number, h is the Plank's constant, ΔS^* is the entropy of activation and ΔH^* is the enthalpy of activation. A plot of log$v$ versus 1/T gave a straight line as shown in Figure 4 with a slope of (E_a/2.303R) and their activation energy values are listed in Table 4. The data given in the Table 4 shows that E_a for the corrosion of carbon steel in HCl solution is higher in inhibiting solution than those in the free acid solution, which is due to the adsorption of investigated inhibitors on the carbon steel surface. Also the higher values of E_a in inhibiting solution might be correlated with the increased thickness of the double layer, which enhances the activation energy of the corrosion process [8]. A plot of log$v$/T against 1/T gives straight lines with a slope value of (ΔH^*/2.303R) and an intercept of [log(R/Nh)) + (ΔH^*/2.303R)] as in Figure 5, from which the values of ΔH^* and ΔS^* were calculated and given in Table 4.

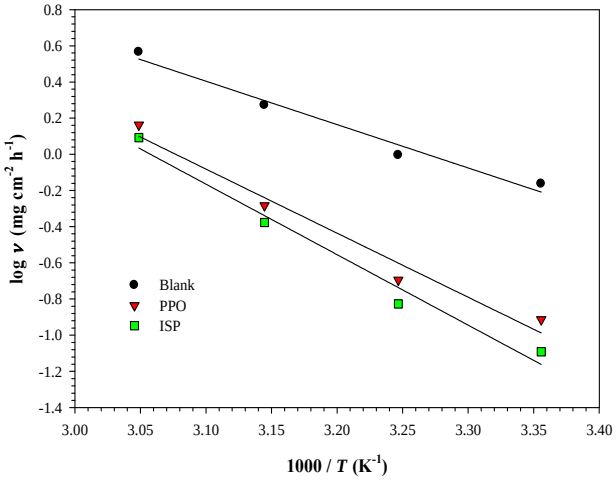

Figure 4: Arrhenius plot for carbon steel dissolution in the absence and presence investigated inhibitors

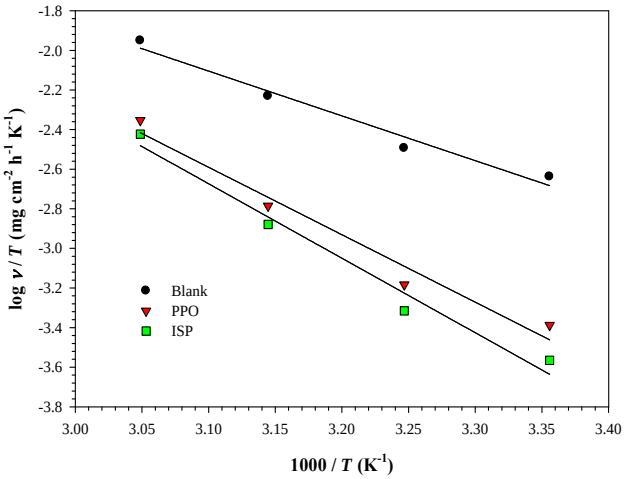

Figure 5: Transition state plot for carbon steel dissolution in the absence and presence investigated inhibitors

Table 4: Activation parameters for carbon steel dissolution in 1.0 mol dm^{-3} HCl in the absence and presence of optimum concentrations (5×10^{-3} mol dm^{-3}) of PPO and ISP inhibitors

Inhibitor	E_a (kJ mol^{-1})	ΔH^* (kJ mol^{-1})	$-\Delta S^*$ (J K^{-1} mol^{-1})
Blank	45.9	43.3	103.6
PPO	67.8	65.2	45.0
ISP	74.6	72.0	25.5

Inspection of these data reveals that the ΔH^* values for the dissolution reaction of carbon steel in 1.0 mol dm^{-3} HCl in the presence of inhibitors are higher than that in the absence of inhibitors. The positive signs of ΔH^* reflect that the dissolution of carbon steel is slow in the presence of inhibitor [9]. The values of E_a and ΔH^* enhance in the presence of inhibitor suggesting that the energy barrier of corrosion reaction increases. This means that the corrosion reaction will further be pushed to surface sites that are characterized by progressively higher values of E_a as the concentration of the inhibitor becomes greater [10]. The values of ΔS^* increase in presence of inhibitor as compared with uninhibited solution (Table 4). This was due to increases in randomness on going from reactants to the activated complex. This might be the results of the adsorption of organic inhibitor molecules from the HCl solution and could be regarded as a quasi-substitution process between the organic compound in the aqueous phase and water molecules at the electrode surface [11]. In this situation, the adsorption of organic inhibitor was accompanied by desorption of water molecules from the surface. Thus the increase in entropy of activation was attributed to the increase in solvent entropy [12].

3.2. Electrochemical measurements

3.2.1. Potentiodynamic polarization measurements

The effect of increased concentration of PPO and ISP on the polarization curves of carbon steel in 1.0 mol dm^{-3} HCl, at 298 K is represented in Figures 6 & 7, respectively. The electrochemical parameters such as corrosion potential (E_{corr}), corrosion current density (i_{corr}), cathodic Tafel constant (β_c), anodic Tafel slope (β_a) and inhibition efficiency (η_p) are calculated and given in Table 5. The η_p was calculated from polarization measurements according to the relation given below [13];

$$\eta_p = \left(\frac{i_t - i_t^o}{i_t}\right)\times 100 \qquad (7)$$

where i and i^o are uninhibited and inhibited corrosion current densities, respectively. It is clear that the i_{corr} decrease with increasing of the inhibitors concentration; this indicates that purine compounds are adsorbed on the metal surface and hence inhibition occurs. The polarization curves (Figures 7 & 8) show that PPO and ISP has an effect on both, the cathodic and anodic slopes (β_c and β_a) and suppressed both cathodic and anodic processes. This indicates a modification of the mechanism of cathodic hydrogen evolution as well as anodic dissolution of iron, which suggest that inhibitor powerfully inhibits the corrosion process of carbon steel, and its ability as corrosion inhibitor is enhanced as its concentration is increased. The suppression of cathodic process can be due to the covering of the surface with monolayer due to the adsorbed inhibitor molecules.

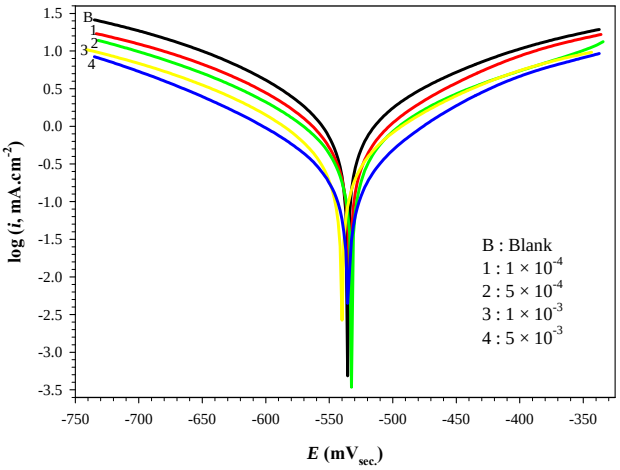

Figure 6: Polarization curves for carbon steel in 1.0 mol dm^{-3} HCl in the absence and presence of various concentrations of PPO

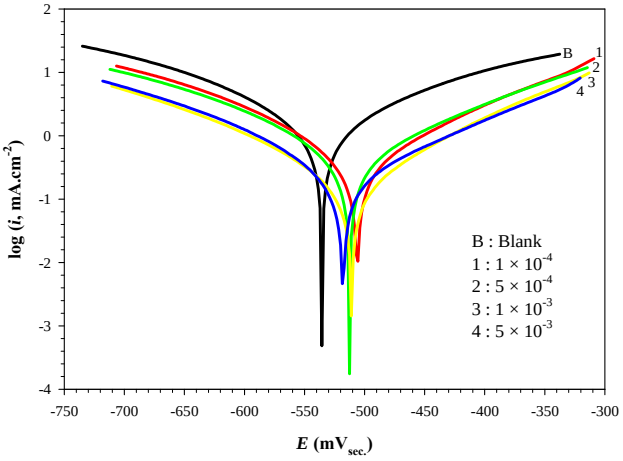

Figure 7: Polarization curves for carbon steel in 1.0 mol dm^{-3} HCl in the absence and presence of various concentrations of ISP

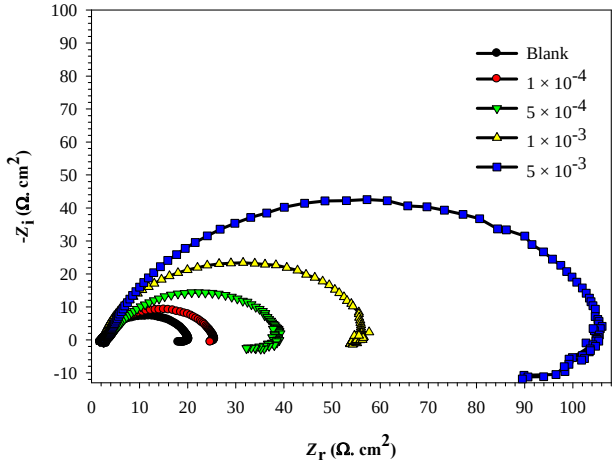

Figure 8: Nyquist plots for carbon steel in 1.0 mol dm^{-3} HCl in the absence and presence of various concentrations of PPO

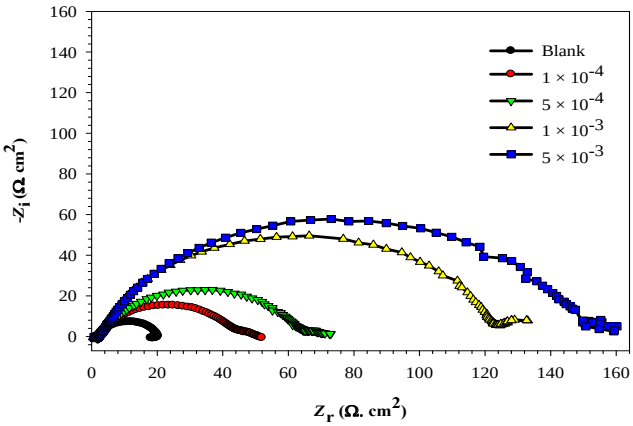

Figure 9: Nyquist plots for carbon steel in 1.0 mol dm^{-3} HCl in the absence and presence of various concentrations of ISP

It can also be seen from Table 5 that the anodic Tafel slope (β_a) decreases in the presence of inhibitors. This observation may be ascribed to changes in the charge transfer coefficient for the anodic dissolution of iron by virtue of the presence of an additional energy barrier due to the presence of adsorbed inhibitor. Further inspection of Table 5 also reveals that E_{corr} values do not show any significant change in the presence of various concentrations of the inhibitor suggesting that PPO and ISP are mixed-type in 1.0 mol dm^{-3} HCl, which influences both metal dissolution and hydrogen evolution [14].

Table 5: Polarization parameters for the corrosion of steel in 1.0 mol dm^{-3} HCl in the absence and presence of various concentrations of PPO and ISP at 298 K

Inhibitor	C (mol dm^{-3})	$-E_{corr}$ (mV$_{SCE}$)	i_{corr} (mA cm^{-2})	β_a (mV dec^{-1})	$-\beta_c$ (mV dec^{-1})	η_p (%)
Blank	0	536	3.0395	242.6	209.6	—
PPO	1×10^{-4}	534	2.1368	216	218	29.7
	5×10^{-4}	532	1.5222	219	201	49.9
	1×10^{-3}	539	0.9798	200	201	67.8
	5×10^{-3}	535	0.5399	144	166	82.2
ISP	1×10^{-4}	506	1.4241	212	212	53.1
	5×10^{-4}	512	0.8043	170	167	73.5
	1×10^{-3}	511	0.3708	143	163	87.8
	5×10^{-3}	518	0.3583	156	144	88.2

3.2.2. Electrochemical impedance spectroscopy (EIS)

Figs. 8 & 9 show the Nyquist plots for carbon steel in 1.0 mol dm^{-3} HCl in the absence and presence of PPO and ISP at 298 K, respectively.

The impedance diagrams consist of a large capacitive loop at high frequencies followed by a small inductive loop at low frequency values. The high frequency capacitive loop is usually related to the charge transfer of the corrosion process and double layer behavior. On the other hand, the low frequency inductive loop may be attributed to the relaxation process obtained from adsorption species like $FeCl_2$ or inhibitor species on the electrode surface [29]. It might be also attributed to the re-dissolution of the passivated surface at low frequencies [30]. Furthermore, the diameter of the capacitive loop in the presence of inhibitors is bigger than that with the uninhibited solution and increases with the inhibitor concentrations. This indicates that the impedance of carbon steel corrosion increases with the inhibitor concentration. The capacitive loops are not perfect semicircles which can be attributed to the frequency dispersion effect as a result of the roughness and inhomogeneous of electrode surface [31,32]. The electrochemical parameters derived from Nyquist plots are calculated and listed in Table 6. The values of charge transfer resistance (R_t) were given by subtracting the high frequency impedance from the low frequency one as follows [15]:

$$R_t = Z_{re}(at\ low\ frequency) - Z_{re}(at\ high\ frequency) \quad (8)$$

The values of electrochemical double layer capacitance (C_{dl}) were calculated at the frequency, f_{max}, at which the imaginary

component of the impedance is maximal ($-Z_{max}$) by the following equation:

$$C_{dl} = (2\pi f_{max} R_t)^{-1} \quad (9)$$

The values of percentage inhibition efficiency (η_i) were calculated from the values of R_t according to the following equation [16]:

$$\eta_i = \left(\frac{R_t - R_t^o}{R_t}\right) \times 100 \quad (10)$$

where R_t and R_t^o are the values of the charge transfer resistance in the presence and absence of inhibitor, respectively.

Table 6: Impedance parameters for the corrosion of steel in 1.0 mol dm^{-3} HCl in the absence and presence of various concentrations of PPO and ISP at 298 K

Inhibitor	C (mol dm^{-3})	R_s (ohm. cm^2)	R_t (ohm.cm^2)	C_{dl} (μF cm^{-2})	θ	η_i (%)
Blank	0	2.4	17.7	455.3	—	—
PPO	1×10^{-4}	2.2	24	331.6	0.272	27.2
	5×10^{-4}	3.7	34	233.7	0.487	48.7
	1×10^{-3}	2.7	53.2	149.5	0.672	67.2
	5×10^{-3}	2.2	98.1	81.1	0.822	82.2
ISP	1×10^{-4}	2.9	43.4	183.3	0.597	59.7
	5×10^{-4}	2.6	65.4	121.6	0.733	73.3
	1×10^{-3}	2.7	120.5	66	0.855	85.5
	5×10^{-3}	2.9	150.7	52.8	0.884	88.4

The impedance data listed in Table 6 indicate that the values of both R_t and η_i are found to increase by increasing the inhibitor concentration, while the values of C_{dl} are found to decrease. This behavior was the result of an increase in the surface coverage by the inhibitor molecules, which led to an increase in the inhibition efficiency. The decrease in C_{dl} values may be considered in terms of Helmholtz model [17]:

$$C_{dl} = \frac{\varepsilon\varepsilon_0}{d} \times S \quad (11)$$

where ε_0 is the permittivity of space (8.854×10^{-12} Fm^{-1}), ε is the local dielectric constant, d is the thickness of the film and S is the surface area of the electrode. In fact, the decrease in C_{dl} values can result from a decrease in local dielectric constant and/or an increase in the thickness of the electrical double layer [18].

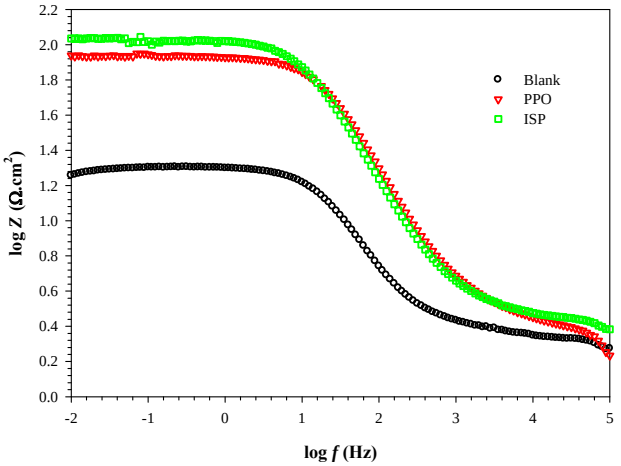

Figure 10: Bode plots for carbon steel in 1.0 mol dm^{-3} HCl in the absence and presence of investigated inhibitors

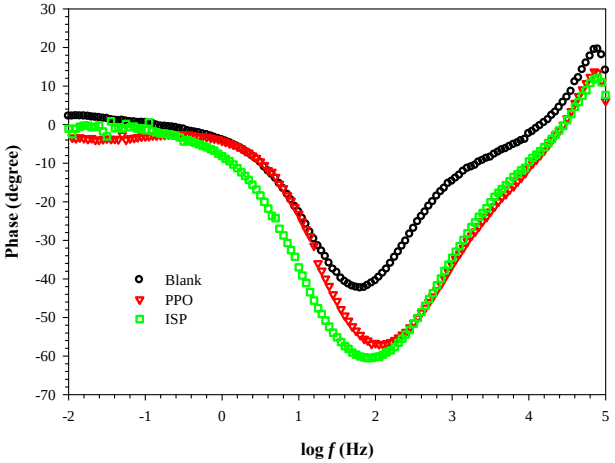

Figure 11: Phase angle plots for carbon steel in 1.0 mol dm^{-3} HCl in the absence and presence of investigated inhibitors

In the Bode plots (Figures 10 & 11) obtained without and with the optimum concentration (5×10^{-3} mol dm^{-3}) of PPO and ISP inhibitors, it was found that the slopes of log$Z$ against log$f$ lines not equal −1, and the spectra consist one time constant. The high-frequency part of the impedance and phase angle describes the behavior of an inhomogeneous surface layer, whereas the low-frequency component depicts the kinetic response to the charge transfer reaction [38]. It is observed that increase maximum phase angle of ISP than PPO, which indicate ISP more inhibition of the corrosion process than PPO. The impedance spectra for the Nyquist plots were analyzed by fitting to the equivalent circuit model shown in Figure 12, which has been used previously to model the steel/acid interface. The circuit comprises a solution resistance R_s shorted by a constant phase element (CPE) that is placed in parallel to the charge transfer resistance R_t.

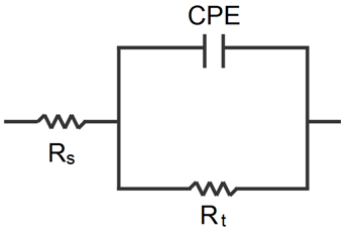

Figure 12: The equivalent circuit model used to fit the impedance data for carbon steel

The value of the charge transfer resistance is indicative of electron transfer across the interface. The use of the CPE, has been extensively described in the literature [19,20] and is employed in the model to compensate for the inhomogeneities in the electrode surface as depicted by the depressed nature of the Nyquist semicircle. The introduction of such a CPE is often used to interpret data for rough solid electrodes. The impedance, Z, of the CPE is:

$$Z_{CPE} = \left[Q(j\omega)^n\right]^{-1} \quad (12)$$

where the coefficient Q is a combination of properties related to different physical phenomena like surface inhomogeneousness, electro-active species, inhibitor adsorption, porous layer formation, etc., j is an imaginary number ($j^2 = -1$), ω is the angular frequency ($\omega = 2\pi f$) and the exponent n has values between −1 and 1. A value of −1 is a characteristic for an inductance, a value 1 corresponds to

a resistor, and a value of 0.5 can be assigned to the diffusion phenomenon [21].

3.4 Explanation for inhibition

The gravimetric and electrochemical results show that, PPO and ISP are efficient for carbon steel corrosion in 1.0 mol dm^{-3} HCl; better performance is seen in the case of ISP ($C_9H_7N_7O_2S$) than PPO ($C_5H_4N_4O$). The agreement between the inhibition efficiencies obtained from gravimetric and electrochemical methods are quite well. The higher inhibition efficiency of ISP can be explained by the presence of the extra imidazole group and S atom in its molecular structure, which are considered to be active centers of adsorption. The presence of such groups in the molecular structure of the inhibitor molecule increases the electron density on adsorption centers and leading to an easier electron transfer from the functional group to the metal surface, producing greater coordinate bonding and higher inhibition efficiency. The inhibition effect of investigating purine inhibitors in HCl solution can be explained as follows: purine inhibitor might be protonated in the acid solution as following:

$$Inh + xH^+ \leftrightarrow [InhH_x]^{x+} \quad (13)$$

Thus, in aqueous acidic solutions, the inhibitor exists either as: (1) neutral molecules or (2) in the form of cations (protonated inhibitor). Generally, two modes of adsorption could be considered. The neutral inhibitor may be adsorbed on the metal surface via the adsorption mechanism, involving the displacement of water molecules from the metal surface and the sharing electrons between the heteroatom's and iron surface. The inhibitor molecules can be also adsorbed on the metal surface on the basis of donor–acceptor interactions between π-electrons of the heterocyclic and vacant d-orbitals of iron surface. In other hand, Cl^- could adsorb on the metal surface, and then the protonated inhibitor may adsorb through electrostatic interactions between the positively charged inhibitor and already adsorbed sulfate ions [22].

4. Conclusions

1) PPO and ISP act as a good inhibitor for the corrosion of carbon steel in 1.0 mol dm^{-3} HCl, and the inhibition efficiency increase with the inhibitor concentration, while decrease with the temperature.
2) The adsorption of the PPO and ISP on the carbon steel surface obeys the Langmuir adsorption isotherm. The values of E_a and ΔH^* enhance in the presence of inhibitor suggesting that the energy barrier of corrosion reaction increases.
3) The potentiodynamic polarization curves indicated that PPO and ISP behave as a mixed-type inhibitor.
4) EIS results indicate that the C_{dl} decrease when these inhibitors are added; this due to adsorption of these inhibitors on the steel surface.

Acknowledgement

The authors are greatly thankful to the Egyptian Petroleum Research Institute (EPRI) fund and support.

References

[1] Shuduan Deng, Xianghong Li, "Inhibition by Ginkgo leaves extract of the corrosion of steel in HCl and H_2SO_4 solutions," Corros. Sci. 55 (2012) 407–415.
[2] H.A. Mohamed, A.A. Farag, B.M. Badran, "Friendly to Environment Heterocyclic Adducts as Corrosion Inhibitors for Steel in Water-Borne Paints," J. Appl. Polym. Sci. 117 (2010) 1270-1278.
[3] Xianghong Li, Shuduan Deng, Hui Fu, Guannan Mu, "Inhibition effect of 6-benzylaminopurine on the corrosion of cold rolled steel in H_2SO_4 solution," Corros. Sci. 51 (2009) 620–634.
[4] M.A. Migahed, A.A. Farag, S.M. Elsaed, R. Kamal, M. Mostfa, H. Abd El-Bary, "Synthesis of a new family of Schiff base nonionic surfactants and evaluation of their corrosion inhibition effect on X-65 type tubing steel in deep oil wells formation water," Mater. Chem. Phys. 125 (2011) 125–135.
[5] T.P. Zhao, G.N. Mu, "The adsorption and corrosion inhibition of anion surfactants on aluminium surface in hydrochloric acid," Corros. Sci. 41 (1999) 1937–1944.
[6] O. O. Xomet, N. V. Likhanova, M. A. D. Anguilar, E. Arce, H. Dorantes, P. A. Lozada, "Synthesis and corrosion inhibition of α-amino acids alkylamides for mild steel in acidic environment," Mater. Chem. Phys., 110 (2008) 344-351.
[7] R. Solmaz, G. Kardas, B. Yazıcı, M. Erbil, "Adsorption and corrosion inhibitive properties of 2-amino-5-mercapto-1,3,4-thiadiazole on mild steel in hydrochloric acid media," Colloids and Surfaces A: Physicochem. Eng. Aspects, 312 (2008) 7–17.
[8] S. Martinez, I. Stern, "Thermodynamic characterization of metal dissolution and inhibitor adsorption processes in the low carbon steel/mimosa tannin/sulfuric acid system," Appl. Surf. Sci. 199 (2002) 83–89.
[9] N. M. Guan, L. Xueming, L. Fei, "Synergistic inhibition between o-phenanthroline and chloride ion on cold rolled steel corrosion in phosphoric acid," Mater. Chem. Phys., 86 (2004) 59-68.
[10] S. S. Abd El Rehim, M. A. M. Ibrahim, K. F. Khalid, "The inhibition of 4-(2′-amino-5′-methylphenylazo) antipyrine on corrosion of mild steel in HCl solution," Mater. Chem. Phys., 70 (2001) 268-273.
[11] M. Sahin, S. Bilgic, H. Yilmaz, "The inhibition effects of some cyclic nitrogen compounds on the corrosion of the steel in NaCl mediums," Appl. Surf. Sci., 195 (2002) 1-7.
[12] B. Ateya, B. E. El-Anadouli, F. M. El-Nizamy, "The adsorption of thiourea on mild steel," Corros. Sci., 24 (1984) 509-515.
[13] Ahmed A. Farag, M.R. Noor El-Din, "The adsorption and corrosion inhibition of some nonionic surfactants on API X65 steel surface in hydrochloric acid," Corros. Sci. 64 (2012) 174–183.

[14] M.A. Quraishi, D. Jamal, "Dianils as new and effective corrosion inhibitors for mild steel in acidic solutions," Mater. Chem. Phys. 78 (2003) 608-613.
[15] Ahmed M. Al-Sabagh, Notaila M. Nasser, Ahmed A. Farag, Mohamed A. Migahed, Abdelmonem M.F. Eissa, Tahany Mahmoud, "Structure effect of some amine derivatives on corrosion inhibition efficiency for carbon steel in acidic media using electrochemical and Quantum Theory Methods," Egyptian Journal of Petroleum 22 (2013) 101–116.
[16] M.A. Migahed, A.A. Farag, S.M. Elsaed, R. Kamal, H.A. El-Bary, "Corrosion inhibition of steel pipelines in oil well formation water by a new family of nonionic surfactants," Chem. Eng. Commun. 199 (2012) 1335-1356.
[17] Ahmed A. Farag, M.A. Hegazy, "Synergistic inhibition effect of potassium iodide and novel Schiff bases on X65 steel corrosion in 0.5 M H_2SO_4," Corros. Sci. 74 (2013) 168–177.
[18] M. Kissi, M. Bouklah, B. Hammouti, M. Benkaddour, "Establishment of equivalent circuits from electrochemical impedance spectroscopy study of corrosion inhibition of steel by pyrazine in sulphuric acidic solution," Appl. Surf. Sci. 252 (2006) 4190-4197.
[19] L. Larabi, Y. Harek, O. Benali, S. Ghalem, "Hydrazide derivatives as corrosion inhibitors for mild steel in 1 M HCl," Prog. Org. Coat. 54 (2005) 256-262.
[20] Popova, E. Sokolova, S. Raicheva, M. Christov, "AC and DC study of the temperature effect on mild steel corrosion in acid media in the presence of benzimidazole derivatives," Corros. Sci. 45 (2003) 33-58.
[21] Hulya Keles, Mustafa Keles, Ilyas Dehri, Osman Serindag, "The inhibitive effect of 6-amino-m-cresol and its Schiff base on the corrosion of mild steel in 0.5 M HCI medium," Mater. Chem. Phys. 112 (2008) 173–179.
[22] F. Bentiss, M. Traisnel, M. Lagrenée, "The substituted 1,3,4-oxadiazoles: a new class of corrosion inhibitors of mild steel in acidic media," Corros. Sci. 42 (2000) 127–146.

Author Profile

Ahmed A. Farag received the B.Sc., Master and Ph.D. degrees in Chemistry from Science Faculty, Al-Azhar University/ Egypt in 2002, 2007 and 2011, respectively. I worked in National Research Center (NRC), Polymers and Pigments Department/Egypt until 2007. Now I am working in Egyptian Petroleum Research Institute (EPRI), Petroleum Applications Department/Egypt from 2007 until now.

Khalid Zakaria, Analysis and Evaluation Department, Egyptian Petroleum Research Institute (EPRI), 1 Ahmed El-Zomor St., Nasr City, 11727, Cairo, Egypt.